Simulating Microbiologically Influenced Corrosion by Depositing Extracellular Biopolymers on Mild Steel Surfaces

*F.L. Roe, Z. Lewandowski, and T. Funk**

ABSTRACT

Electrochemical properties of corroding mild steel (MS) surfaces were measured in real time using three closely spaced microelectrodes. Dissolved oxygen, pH, and ion currents were mapped simultaneously and noninvasively above a MS coupon partially coated with biopolymer gels. Calcium alginate (Ca-Alg [an extracellular biopolymer containing carboxylate functional groups]) and agarose (one without carboxylate functional groups) were tested. Corrosion occurred at approximately the same rate under the two biopolymer spots on the same coupon. Corrosion rates under these biopolymers were ≈ 4 mpy in a weak saline solution. Results suggested corrosion was not influenced by chemical properties of the biopolymer but possibly was controlled by oxygen reduction in noncoated regions of the coupon (i.e., a differential aeration cell).

KEY WORDS: biopolymers, dissolved oxygen, microbiologically influenced corrosion, microelectrode, mild steel, pH, scanning vibrating electrode

INTRODUCTION

Bare mild steel (MS) corrodes in dilute saline solutions with no pronounced polarization. The metal rarely passivates, and corrosion rates normally increase with corrosion potentials.[1] Oxygen reduction normally is the rate-limiting step because of diffusional or mixed diffusion-reaction control.[2]

Microorganisms growing on water-immersed metal surfaces form biofilms that are held together by extracellular polymeric substances (EPS) or biopolymers. Biofilms on MS often are associated with microbiologically influenced corrosion (MIC), which is a more aggressive and localized form of corrosion.[3]

Widespread evidence indicates many extracellular polymers produced by bacteria are acidic and contain functional groups that easily bind metal ions.[4-7] It is plausible that complexation of metal ions by these polymers in biofilms may speed corrosion.

However, White, et al., found no accumulation of iron or other metals in EPS from biofilms growing on corroding type 304 (UNS S30400)(1) stainless steel (SS).[8] The accelerated corrosion was attributed to inhomogeneous distribution of biofilm at the metal surface, resulting in areas of differing cathodic activity. This was consistent with a differential aeration cell, where areas covered with biofilm exhibited lowered oxygen concentrations and became anodic while those with less biofilm were exposed to higher oxygen concentrations and became cathodic.

Iverson proposed that natural heterogeneous distribution of biofilm on a metal surface under aerobic conditions results in a differential aeration cell.[9] Hernandez-Duque, et al., reported a decrease in the corrosion rate of MS in the presence of a uniform layer of biofilm.[10] This decrease was attributed to respiration of the biofilm, which resulted in a decline in oxygen concentration at the metal surface and an

Submitted for publication May 1995; in revised form, November 1995.

* Center for Biofilm Engineering, Montana State University, Bozeman, MT, 59717.

(1) UNS numbers are listed in *Metals and Alloys in the Unified Numbering System*, published by the Society of Automotive Engineers (SAE) and cosponsored by ASTM.

0010-9312/96/000165/$5.00+$0.50/0

associated decrease in the rate of cathodic reduction of oxygen. He duplicated this observation in synthetic seawater with *Pseudomonas sp.* S9 and *Serratia marcescens*.[11] Adhesion of bacteria to the surface also appeared to be a factor in corrosion inhibition. Smith, et al., reported that agar-coated steel (artificial biofilm) also produced a very high polarization resistance and low corrosion rate.[12]

Quantification of corrosion has been limited largely to measuring average values of corrosion-related properties at actively corroding surfaces. With the introduction of areal mapping of chemical characteristics near surfaces using microelectrodes, including the scanning vibrating electrode (SVE), pinpointing corrosion and correlating it with other surface characteristics is possible. Lewandowski, et al., showed corrosion occurs rapidly under a localized spot of calcium alginate (Ca-Alg) biopolymer gel devoid of living organisms.[13] The observed corrosion was consistent with an active differential aeration cell or a metal concentration cell.

In a differential aeration cell, the region that exhibits corrosion also inhibits oxygen transport to the metal surface. Oxygen reduction occurs preferentially in gel-free regions. In a metal concentration cell, the high concentration of carboxylate functional groups in the gel may promote metal complexation and increase corrosion in the biopolymer-coated region. Thus, two mechanisms are possible: a metal concentration cell arising from complexation of metal ions in regions covered with biopolymer or an oxygen concentration cell (differential aeration cell) resulting from inhibition of oxygen transport to the metal surface below the biopolymer.

The present work tested the hypothesis that corrosion of MS under a Ca-Alg gel spot is promoted by complexation of corrosion products by alginate carboxylate functional groups. Alginates are naturally occurring copolymers consisting of linear chains of 1,4 linked β-D-mannuronic and α-L-guluronic acid units. Tests were run by comparing two spots of alginate gel with different surface densities and by comparing two gel spots with the same surface density, but with one gel spot consisting of Ca-Alg (with carboxylate functional groups) and the second spot consisting of agarose (without carboxylate functional groups). Agarose, a naturally occurring polymer, consists of repeating subunits of agarabiose, an alternating 1,3 linked β-D-galactopyranose and 1,4 linked 3,6-anhydro-α-L-galactopyranose structure.

Comparisons were made by mapping electrochemical characteristics directly above the biopolymer-spotted coupons using three closely spaced microelectrodes. Dissolved oxygen (DO), pH, and ion currents were scanned simultaneously and noninvasively above the biopolymer-coated regions. From maps of these variables, a portrait of biopolymer-enhanced corrosion was constructed.

MATERIALS AND METHODS

Oxygen Microelectrode

The oxygen microelectrode was a Clarke-type electrode with an internal silver-silver chloride (Ag-AgCl) half-cell reference and a silicone polymer diffusion membrane. A description of its construction has been given elsewhere.[14]

pH Microelectrode

The pH microelectrode was constructed using a modified pH-sensitive liquid ion exchange cocktail.[15] The cocktail, modified from the original composition, was: 1 wt% N,N-dioctadecylmethylamine ($[CH_3(CH_2)CH_{17}]_2NCH_3$); 67.0 wt% 2-nitrophenyl octyl ether ($2\text{-}NO_2C_6H_5O[CH_2]_7CH_3$); 0.3% sodium tetraphenylborate ($[C_6H_5]_4B^-Na^+$); and 31.7 wt% polyvinyl chloride (PVC) high molecular weight (Fluka 81392†). All ingredients were dissolved in 200 µL of tetrahydrofuran ($[CH_2]_4O$).

A lead glass tube (2 mm [0.079 in.] outer diam [OD]) was drawn to a fine capillary (< 20 µm diam). The tip was silanized using a 10% trimethylchlorosilane ($[CH_4]_3SiCl$), 90% carbon tetrachloride (CCl_4) solution. The membrane was applied to the tip of the microcapillary by placing it in the ion exchange cocktail for ≈ 2 s. The electrode was allowed to dry, with the tip up, in a dust-free environment for 24 h. Once the electrodes were cured, they were back-flled with a solution of 50 mM potassium dihydrogen phosphate (KH_2PO_4) and 300 mM potassium chloride (KCl) adjusted to pH 7 and degassed. The last step was to insert a Ag-AgCl reference electrode into the back-filled solution.

Scanning Vibrating Electrode

When corrosion occurs, ion currents generally develop between the anodic and cathodic sites on the metal surface. Weak electric fields generated by these ion currents can be measured and mapped using a SVE.[16]

The SVE was a glass-sheathed platinum microelectrode vibrated in the vertical plane through a 15-µm to 30-µm excursion at 100 Hz to 200 Hz. The SVE, along with a nearby stationary reference platinum wire, constituted a complete circuit that measured potential gradients at different locations in the corrosion-generated electric field. A high-impedance alternating current (AC) amplifier and lock-in amplifier (LIA) conditioned the signal, allowing measurement of µV-level AC signals induced in the SVE circuit. The mechanical drive unit for the SVE (Figure 1) used a small loudspeaker[17] activated by the reference output signal from the LIA. The electrode signal was preconditioned using a specially equipped high-

† Trade name.

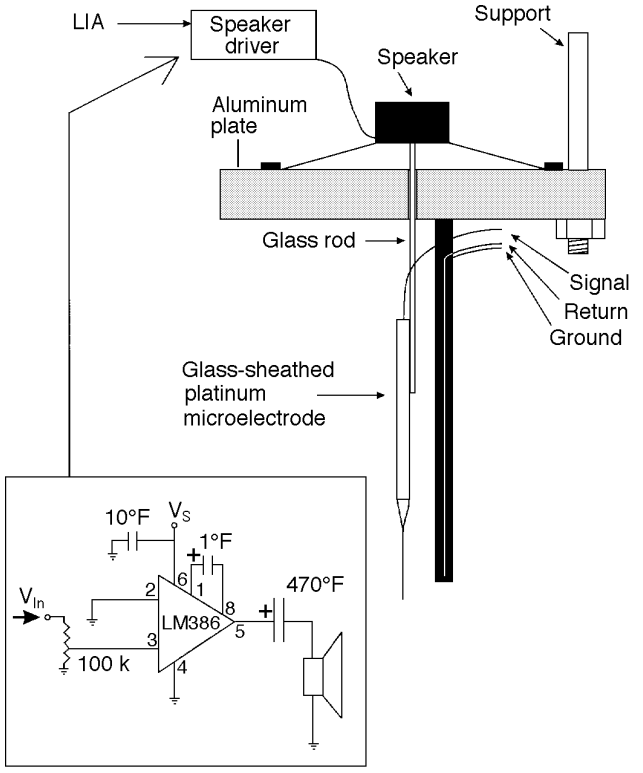

FIGURE 1. *Drive unit for the SVE, whre V_{in} is a lock-in frequency, AC voltage is supplied by the LIA, and V_S is a positive direct current (DC) supply voltage used to power the amplifier chip.*

impedance AC amplifier (Applicable Electronics Model 100 Differential Input Preamplifier†) with a gain of 100 (V_{out}/V_{in}). The amplifier had provisions for conveniently testing the electrode and platinizing the tip. The amplified signal was fed back to the LIA.

Positioning Table and Data Collection

A computer-controlled positioning table was used to move the sample under the stationary microelectrodes. Movement of the table and concurrent collection of quantitative data from all three probes were coordinated using a personal computer. A 12-bit analog-to-digital (A/D) conversion board and custom software were used for data collection.

Biopolymer Solutions

Alginic acid, sodium salt (Na-Alg) of medium viscosity (Sigma A2033†), and agarose (Sigma A4108†) were used as received. Properties of the alginic acid used have been described previously.[13] The agarose gel was noncharged, porous, resistant to bacterial degradation, and did not require counterions for stability.[18] Solutions (wt%) were prepared by dissolving the appropriate weight of polymer in demineralized water. For example, 3% sodium alginate (Na-Alg) solution was prepared by dissolving 3.0 g of the sodium salt of alginic acid in 75 mL (4.65 in.^{3}) of demineralized water and diluting to 100 mL (6.20 in.^{3}).

Coupon Preparation and Procedures

Type C1018 (UNS G10180) MS coupons (1 cm [0.625 in.] diam) were obtained from a commercial supplier. They were embedded in drilled-out PVC plug fittings using Buehler Epoxide resin 20-8132-032† and hardener 20-8132-008†. Release-agent 20-8185-008† was used to prevent sticking to other surfaces. Various epoxy resins were tried, and this type resulted in fewer cases of crevice corrosion at the coupon edges.

Coupon surfaces were polished using wet silicon carbide (SiC) and aluminum oxide (Al_2O_3) papers of 400-; 600-; 1,000-; 1,200-; 1,500; and 2,000-grit. A final polish to a mirror finish was accomplished using wet crocus paper (iron oxide [Fe_2O_3]).

Biopolymer spots were placed on the coupons by injecting 5.0 µL of the appropriate solution onto the surface, spreading it to a diameter of 2 mm to 3 mm (0.079 in. to 0.118 in.) using a plastic fiber, and letting it partially dry under a stream of warm air. When two spots were placed on the coupon, they were 3 mm apart and along a line parallel to the X scan axis (Figure 2).

A plug with the prepared coupon was mounted in the bottom of a square polycarbonate vessel with transparent sides. The vessel was fastened to the X-Y micropositioning table. Before adding electrolyte, the three microelectrodes (DO, pH, and SVE) were positioned ≈ 140 µm above the coupon and 700 µm apart along a line parallel with the X scan axis. This was accomplished using manual micromanipulators and viewing the microelectrodes through the transparent vessel sides using a stereoscopic dissecting microscope.

After positioning the microelectrodes, a drop of 50 mM calcium chloride ($CaCl_2$) solution was placed on the partially dried alginate for 10 s to convert the Na-Alg to Ca-Alg. Immediately after, 200 mL (6.76 oz) of an electrolyte (1 mM sodium chloride [NaCl] + 1 mM sodium sulfate [Na_2SO_4] in demineralized water) was added to the vessel. The SVE was calibrated using the procedure described by Jaffe and Nuccitelli.[16] In this procedure, the SVE is positioned a known distance from the tip of a glass pipet containing a Ag-AgCl reference electrode. A voltage is applied between it and ground, resulting in a measured current of ~ 100 nA. From the geometry of the arrangement and the assumption of a spherically symmetrical current distribution at the tip of the pipet, the relationship between response of the LIA and current density at the SVE tip can be calculated.

Scanning was initiated immediately after calibration of the SVE. The entire coupon surface was scanned, resulting in a separate square matrix of data for each microelectrode. The table was stepped

at 700-µm intervals along a transect in the X direction. Multiple parallel transects 700 µm apart were taken to form the mapping grid. Table movement, settling time, and data collection took ≈ 3 s for each step. Consequently, for each grid point, all three microelectrode measurements were made within 9 s.

Since the spatial orientation of the electrodes was well-defined, the matrices could be overlaid and microelectrode specific surface activities correlated.

EXPERIMENTS

Three experiments were conducted to test the hypothesis that corrosion of MS under Ca-Alg gel is controlled by complexation of corrosion products by alginate carboxylate functional groups (Figure 2). In each experiment, near-surface DO, pH, and ion currents were measured. The ion currents, measured with the SVE, were a measure of corrosion rate.

The experimental and control conditions were:

— In Experiment 1, a single region of a MS coupon was spotted with 3% Ca-Alg.

— In Experiment 2, two adjacent 0.05-cm^2 (7.75 x 10^{-3} in.^{2}) biopolymer spots were placed on the coupon. The first spot (3% alginate), had a surface density of 30 g/m^2, while the surface density of the second spot (0.3% alginate) was 3.0 g/m^2. Therefore, the surface density of carboxylate groups for the first spot was 10 times that of the second spot.

— In Experiment 3, two adjacent 0.05-cm^2 regions of a coupon were coated with biopolymer. Both regions, one with 1.5% agarose and one using 1.5% alginate, had surface densities of 15 g/m^2.

— In Control 1, the active area of a commercial DO probe was coated with 2% Na-Alg solution. The coating was allowed to dry 5 min before the probe was immersed in 0.5 M $CaCl_2$ solution. Oxygen concentrations were measured before and after the treatment in air-saturated water at room temperature.

— In Control 2, the rate of oxygen reduction again was measured, this time at the surfaces of bare platinum wires coated with Ca-Alg. One set of wires was coated with 2% Na-Alg, allowed to dry 30 min, and immersed in 0.1 M $CaCl_2$. The second set of wires was coated identically with 2% Na-Alg and immediately immersed in 0.1 M $CaCl_2$. Each wire was dipped in air-saturated tap water, a direct current potential of –0.75 V was applied, and the current was measured vs a carbon anode.

RESULTS

Experiment 1

This experiment confirmed that corrosion on MS preferentially takes place under biopolymer-coated regions, while cathodic activity is limited to uncoated regions.[13] A strongly anodic region was detected with the SVE above the alginate biopolymer spot on the coupon (Figure 3). This region exhibited low pH and a localized maximum in oxygen concentration. Measurements taken from the rest of the coupon indicated a pronounced cathodic region (SVE) with high pH and essentially zero oxygen concentration. Most of the observable corrosion was located in the biopolymer-coated region.

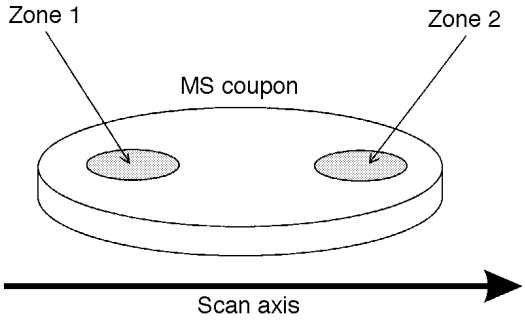

Experiment	Zone 1	Zone 2
1	Bare metal	Ca-Alg (30 g/m^2)
2	Ca-Alg (30 g/m^2)	Ca-Alg (3.0 g/m^2)
3	Agarose (15 g/m^2)	Ca-Alg (15 g/m^2)

FIGURE 2. *Spot placement on MS coupon.*

Each data point recorded for the SVE was a measure of current density in µA/cm^2 for a single scan grid element. Summing the SVE data measured above the biopolymer spot and multiplying by the area per grid element furnished the total current above this specific region (Equation [1]). The total current from the biopolymer-spotted region was highly anodic (Table 1).

$$\text{Total anodic current} = \left(\frac{\text{cm}^2}{\text{grid element}}\right) \times \sum_{\substack{\text{anodic grid}\\ \text{elements}}} \left(\frac{\text{current}}{\text{cm}^2}\right) \quad (1)$$

The same procedure was used for measuring the total current from the remaining area of the coupon, which was cathodic.

Experiment 2

The results expected from the hypothesis was that the region of higher alginate density (covered by 3% alginate) would exhibit more rapid corrosion than that covered by 0.3% alginate. Instead, both spots behaved similarly and provided similar contours (Figure 4). Table 2 shows total ion currents above both spots after 4 h. Total ion currents were calculated as in Experiment 1.

Experiment 3

Because agarose has no carboxylate functional groups, it was hypothesized that corrosion would be significantly less under this region than under a

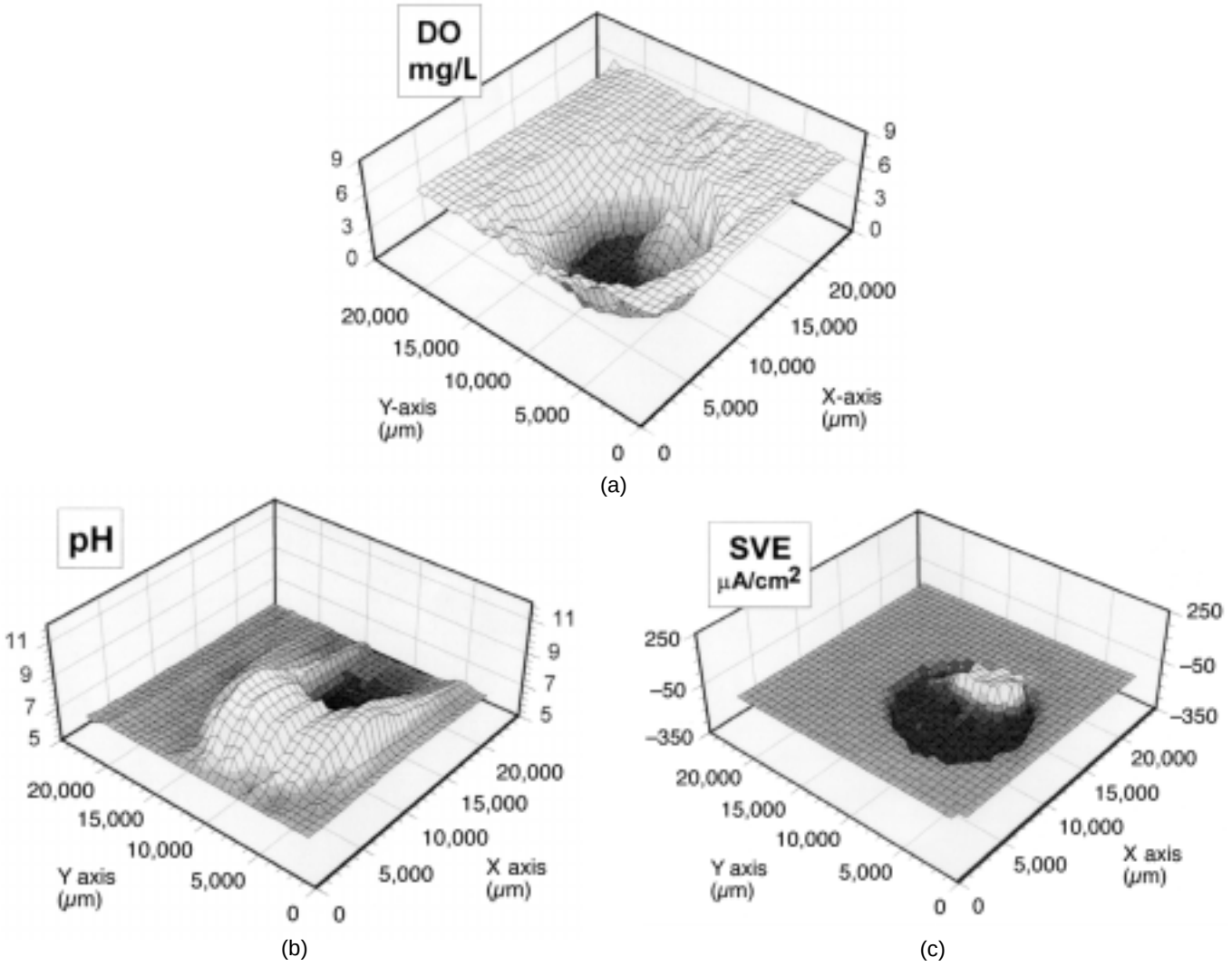

FIGURE 3. *Maps of (a) DO, (b) pH, and (c) current density (SVE) above a corroding MS coupon with a 0.075-cm² (0.012-in.²) spot of Ca-Alg (20 g/m²). The larger raised or depressed circular region in each plot (approx diam. = 15,000 μm [0.625 in.]) represents the entire exposed area of the MS coupon.*

similar region of caboxylate-rich alginate. Again, the hypothesis was disproved. Both biopolymer spots behaved similarly and provided similar contours (Figure 5). Table 2 shows total anodic currents above both spots, as in Experiment 2. Total anodic currents were calculated in the same manner as in the first two experiments.

Corrosion rates were calculated from total spot currents and spot areas (Equation [2]):

$$r_{corr} = \frac{i \times 3{,}600\,s/h \times 27.93\,g\ Fe/equivalent}{96{,}490\,coul/equivalent \times A} \qquad (2)$$

where r_{corr} is the corrosion rate measured in g Fe/h/cm², i is the current in coul/s, and A is the area in cm². The minimum r_{corr} was calculated to be 9.17 x 10^{-6} g Fe/h/cm². Based on a density of 7.9 g/cm³ for MS, this was equivalent to ≈ 4 mpy.

It was speculated that partially drying the biopolymer on the surface before crosslinking it with calcium ion might have created an artifact that was atypical of a true biofilm (i.e., the rate of penetration of oxygen through the dried and rehydrated biopolymer may have been significantly slower than that through biopolymer maintained in a hydrated state). Two experiments were conducted to test this possibility.

Control 1

The measured oxygen concentration was expected to be a Fick's Law function of the bulk water oxygen concentration (oxygen concentration at the electrode surface was virtually zero) and the combined diffusional resistance due to the probe membrane and alginate coating. Before treatment,

the measured concentration was 6.34 mg O_2/L. After treatment, it was 5.6 mg O_2/L. Apparent reduction in oxygen concentration from increased diffusional resistance of the dried and rehydrated alginate coating was ≈ 12%. The alginate coating provided less resistance to oxygen transport than the DO probe membrane.

Control 2

The dried Na-Alg produced films on platinum wire which, when immersed in air-saturated water, showed an average current (3 wires) of 287 nA ± 15 nA. The moist Na-Alg produced films resulting in an average current (3 wires) of 321 nA ± 20 nA. The rate of oxygen transport for the dried and rehydrated alginate coated wires was ≈ 11% less than for freshly coated wires.

While there was a slight difference in oxygen permeability between dried/rehydrated and hydrated alginate films, this difference did not affect conclusions of the study.

DISCUSSION

Corrosion activity, surface oxygen concentrations, and associated pH differences presented a consistent picture in Experiments 1 through 3. The local interfacial equilibrium chemistry could be represented simplistically by Equations (3) through (6):

Anodic region:

$$Fe^0 \rightarrow Fe^{2+} + 2e^- \quad (3)$$

Cathodic region:

$$2e^- + H_2O + 1/2\,O_2 \rightarrow 2OH^- \quad (4)$$

Further oxidation:

$$2Fe(OH)_2 + 1/2\,O_2 \rightarrow Fe_2O_3 + 2H_2O \quad (5)$$

Hydrolysis:

$$Fe^{2+} + 2H_2O \rightarrow Fe(OH)_2 + 2H^+ \quad (6)$$

The first experiment replicated the findings of Lewandowski, et al., by showing that corrosion preferentially occurred under the alginate biopolymer-coated region of the MS coupon.[13] Anodic and cathodic currents were measured independently by summing over the appropriate scan grid elements. For any electrochemical cell, such as corrosion occurring on a MS coupon, the total anodic current (Equation [3]) should equal the cathodic current (Equation [6]). This did not happen in the first experiment, probably because of the coarse scan grid used. As the SVE scanned the surface, it detected a relatively uniformly distributed cathodic current. Because corrosion occurred at localized areas of the coupon in the early stages and the scan step size was coarse, some of the anodic sites were missed. As corrosion sites matured, they spread to form broader sources of anodic current, which were less likely to be missed. Anodic and cathodic currents became more equal in later stages of the experiment, consistent with this hypothesis.

TABLE 1
Comparison of Anodic and Cathodic Ion Currents Above a Ca-Alg Gel Spot (0.075 cm²) on MS Coupon

Time After Start of Experiment (h)	Anodic Current (μA)	Cathodic Current (μA)
0.3	1.72	–4.57
1.6	3.18	–4.64

TABLE 2
Comparison of Anodic Ion Currents Above Two Adjacent (0.05 cm²) Gel Spots on MS Coupon

	Time After Start of Experiment (h)	Anodic Current Spot 1 (μA)	Anodic Current Spot 2 (μA)
Spot 1 = 3% Ca-Alg Spot 2 = 0.3% Ca-Alg	4	0.76	0.81
Spot 1 = 1.5% Agarose Spot 2 = 1.5% Ca-Alg	0.72	1.08	0.58

Experiments 2 and 3 addressed the possibility that carboxylate functional groups complexed with corrosion products and controlled the corrosion location. Alginic acid is a naturally occurring linear polymer consisting of mannuronic and guluronic acid subunits. Each acid subunit contains a single carboxylic acid functional group. The affinity of Ca-Alg for divalent metal ions is documented.[19-21] It was possible that, in the presence of these complexing alginate gels, oxidation of the MS was enhanced. This is represented by expansion of Equations (4) and (5):

$$Alg - Ca + Fe^{2+} \rightarrow Alg - Fe + Ca^{2+} \quad (7)$$

$$Alg - Fe + 1/4\,O_2 + H_2O \rightarrow 1/2\,Fe_2O_3 + 2H^+ + Alg^{2-} \quad (8)$$

$$Alg^{2-} + Ca^{2+} \rightarrow Alg - Ca \quad (9)$$

In Equations (7) through (9), Alg represents binding sites for divalent metal ions in the alginate gel polymer. If so, the Alg-complexed ferrous ion

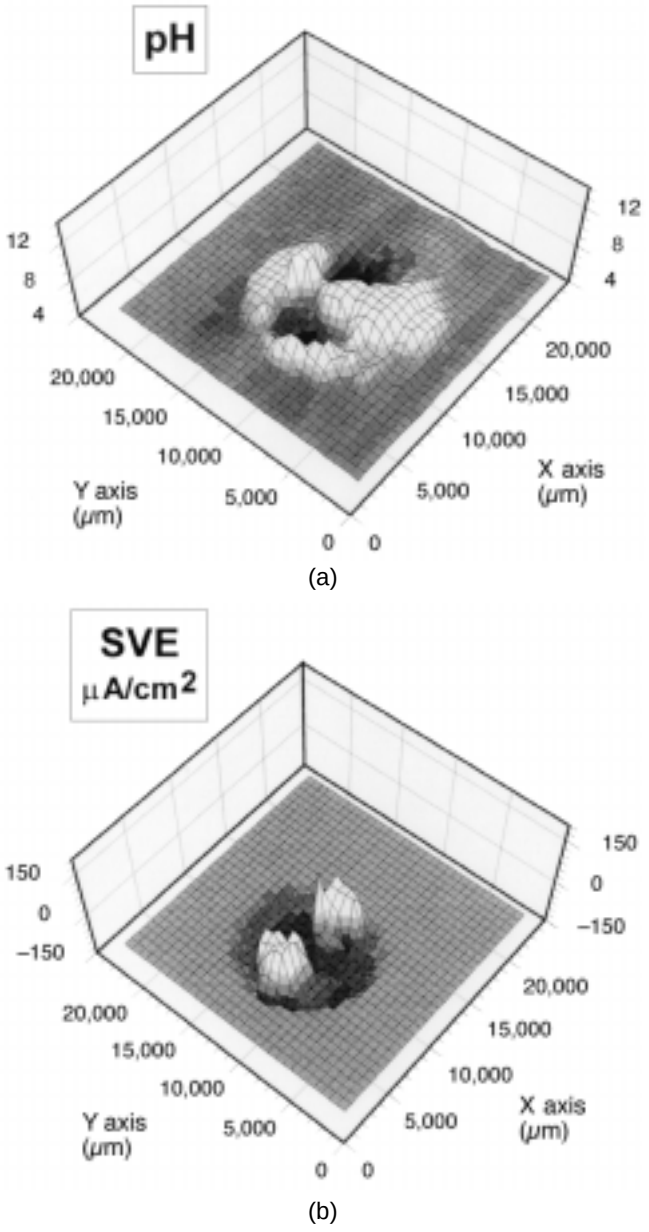

FIGURE 4. *Maps of (a) pH and (b) current density (SVE) above a corroding MS coupon with two 0.05-cm² spots of Ca-Alg: (left) 3.0 g/m² and (right) 30 g/m². The larger raised or depressed circular region in each plot (approx diam. = 15,000 μm [0.625 in.]) represents the entire exposed area of the MS coupon.*

could have oxidized more rapidly than the soluble hydrated ion, a catalytic effect. Or, from mass action considerations, the decreased ferrous ion concentration could have promoted corrosion underneath the alginate coating. In either case, it was hypothesized that the presence of carboxylate functional groups may have caused enhanced corrosion under the alginate biopolymer gel.

Experiments 2 and 3 provided evidence that rejected this hypothesis. Both experiments showed that carboxylate functional groups did not enhance oxidation under a biopolymer gel. Even when the surface densities of alginate gel and the carboxylate functional groups were increased by a factor of 10, the corrosion rate, as represented by SVE-measured anodic ion currents, was not increased (Table 2). Likewise, when carboxylate functional groups were entirely absent (when agarose was substituted for alginate), there was no decrease in corrosion rate (Table 2). If anything, the corrosion rate was slightly greater under the agarose.

If the structure or composition of the biopolymer did not determine the rate of corrosion, then the rate-determining factor must have been something else. It was entirely possible that the oxygen reduction reaction in the uncoated regions of the coupon limited the reaction rate.

Anodic and cathodic sites were expected to develop on MS surfaces in the presence of an electrolyte. However, it was not immediately clear why location of the corrosion sites was dictated by the location of biopolymer gel spots. The process could be explained hypothetically by the presence of a differential aeration cell. The alginate coating on the coupon may have limited oxygen transport to the metal surface and, hence, created a differential aeration cell.[22] This would have encouraged oxygen reduction, hydroxide ion generation, and cathodic behavior in the biopolymer-free areas. In the alginate-coated region, anodic behavior and corrosion would have resulted. This appeared to have been the case, even though oxygen transport to metal below the alginate coating was expected to be nearly the same as that in the uncoated region, that is:

— The system was stagnant, and there was little or no convective mixing;

— The alginate coating was thin, on the order of 50 μm; and

— For small molecules, diffusion coefficients in Ca-Alg gels were nearly the same as in water.[23]

While it was somewhat surprising that such minute differences in oxygen concentration could be responsible for controlling the corrosion process, there was precedent. LaQue demonstrated that small differences in oxygen mass transport, such as those created on rotating disks in aerated water, can produce differential aeration cells resulting in pronounced corrosion.[24] Regions close to the center of the disk, where diffusional resistance to oxygen transport was greatest, corroded, while those near the edge were free of corrosion. Consequently, the small differences in oxygen gradients in the present system could have produced differential aeration cells similar to those seen by LaQue. In addition, the present experiments comparing oxygen transport at commercial oxygen electrodes and platinum wires, with and without alginate film coatings, showed diffusion rates were affected measurably, albeit only slightly.

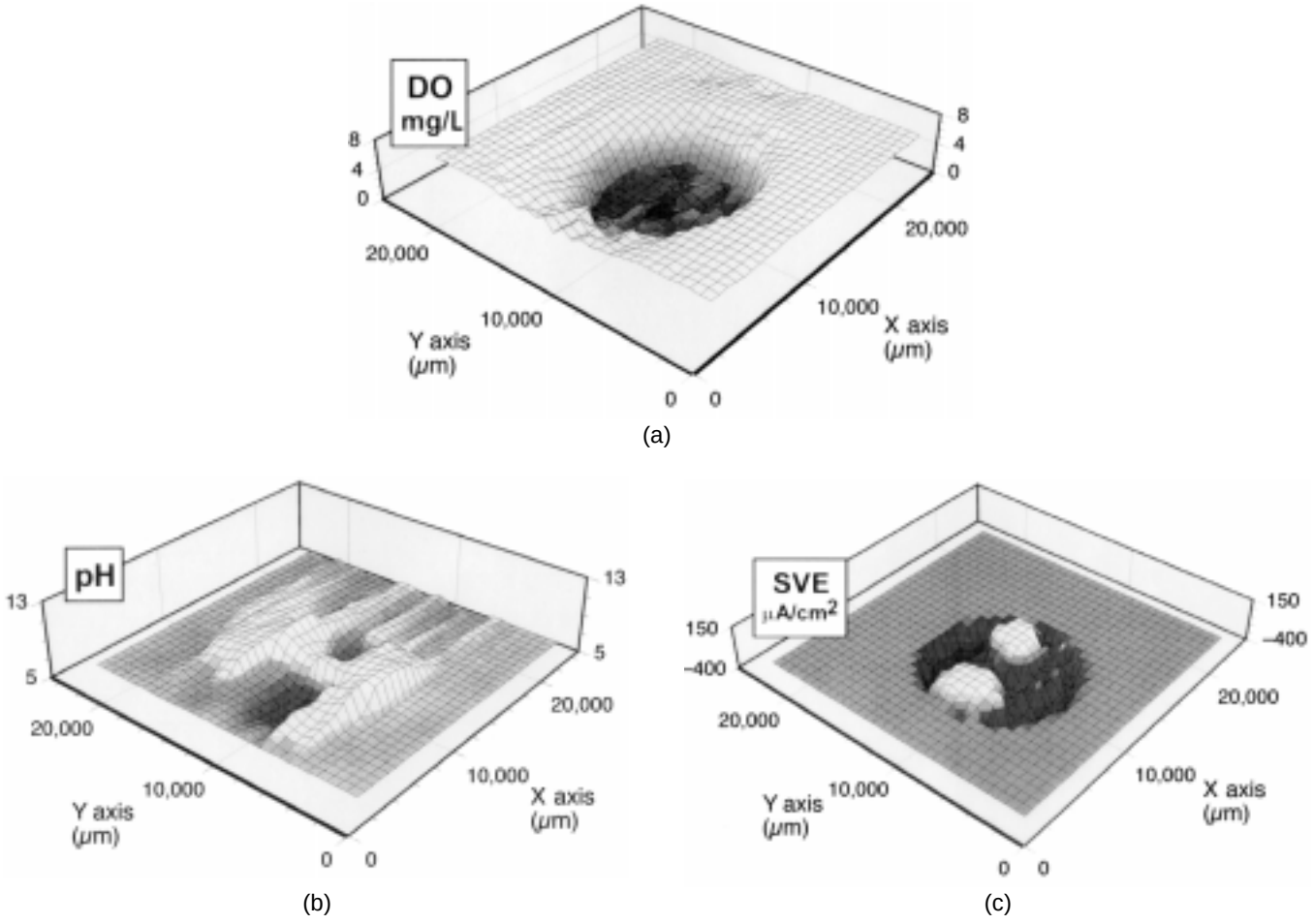

FIGURE 5. *Maps of (a) DO, (b) pH, and (c) current density (SVE) above a corroding MS coupon with two 0.05-cm² spots of biopolymer: (left) 15 g/m² agarose and (right) 15 g/m² Ca-Alg. The larger raised or depressed circular region in each plot (approx diam. = 15,000 μm [0.625 in.]) represents the entire exposed area of the MS coupon.*

Solutions of isolated acidic EPS from *P. atlantica* (a marine bacterial isolate), alginic acid, and gum arabic have been shown to have a wide range of affects on the dissolution rate of copper from copper surfaces.[4-5] These observations support the assertion that chemical composition and binding tendencies of polysaccharides may be important in determining the rate and extent of corrosion from biofilms. However, solutions of EPS, while exhibiting some physical structure as most colloidal suspensions do, are not the same as intact biofilm EPS. The structural integrity of a biofilm necessitates that its EPS be fixed in place in a matrix of interconnected elements that maintain their relationships to each other and to the underlying substratum. Because they are organized differently, biofilm EPS and solution EPS have potentially different activities at metal surfaces. With colloidal suspensions of EPS, there is constant movement of particles toward and away from the surface. These particles undoubtedly adsorb to the surfaces under all naturally occurring conditions. However, the extent to which this is irreversible is unknown. At one extreme, there is no adsorption, and exposure to fresh uncomplexed biopolymer constantly brings new binding agents into contact with the surface. At the other extreme, EPS is bound irreversibly to the surface, especially when there is a strongly adherent conditioning film such as some glycoproteins. The latter case is somewhat analogous to biofilm EPS, but the biopolymer layer may not extend as far into the bulk solution.

The significant dissolution rates of metal substrata observed may be marginally relevant to the processes occurring underneath biofilms and may even be an artifact of the isolation methods used. This is not to say that chemical composition of EPS is not a factor in dissolution of metallic substrata, but that it may not be as significant as the differential aeration cells created by heterogeneously distributed biofilm.

White, et al., reported that the most likely mechanism for facilitated corrosion in their system

involved generation of areas of differing cathodic activity through the heterogenous distribution of bacteria and EPS on their coupons.[8] They strongly suggested that "accumulations of materials elaborated (i.e., generated) by bacteria can facilitate corrosion." The present results support this suggestion and further show that living organisms are not required.

CONCLUSIONS

❖ Corrosion was enhanced under organism-free biopolymer spots on MS, confirming the results of Lewandowski, et al.[13]
❖ Carboxylate functional groups were not necessary to enhance this corrosion, implying that biopolymer chemical structure did not control corrosion rates on the MS coupons.
❖ Corrosion rates were comparable for two different biopolymers (with and without carboxylate groups), suggesting that oxygen reduction may have been the rate-limiting step.
❖ These results may have significant implications for the prevention of MIC on MS. If a biopolymer alone can stimulate corrosion, then merely killing the microorganisms that form the biofilm will not stop MIC. Because differential aeration cells caused by heterogeneously distributed biofilms may be one of many mechanisms responsible for corrosion of MS, the relative contribution of each to MIC must be evaluated.

ACKNOWLEDGMENTS

The authors acknowledge support of the National Science Foundation under cooperative agreement EEC-8907039.

REFERENCES

1. H. Uhlig, Corrosion and Corrosion Control (New York, NY: John Wiley and Sons, 1971), p. 92.
2. A. Bonnel, F. Dabosi, C. Deslouis, M. Duprat, M. Keddams, B. Tribollet, J. Electrochem. Soc. 130 (1983): p. 753.
3. D. Pope, D. Duquette, P.C. Wayner Jr., H.J. Arland, Microbiologically Influenced Corrosion: A State of the Art Review, MTI Publication No. 13 (Columbus, OH: Materials Technology Institute of the Chemical Process Industries Inc., 1984), p. 21-25.
4. G.G. Geesey, L. Jang, J.G. Jolley, M.R. Hankins, T. Iwaoka, P.R. Griffiths, Water Sci. Technol. 37, 11-12 (1988): p. 161.
5. J.G. Jolley, G.G. Geesey, M.R. Hankins, R.B. Wright, P.L. Wichlacz, Surf. Interf. Anal. 11 (1988): p. 371.
6. J.G. Jolley, G.G. Geesey, M.R. Hankins, R.B. Wright, P.L. Wichlacz, Appl. Surf. Sci. 37 (1989): p. 469.
7. T. Ford, R. Mitchell, Adv. Microb. Ecol. 17 (1990): p. 231.
8. D.C. White, D.E. Nivens, P.D. Nichols, A.T. Mikell, B.D. Kerger, J.M. Henson, G.G. Geesey, C.K. Clarke, "Role of Aerobic Bacteria and Their Extracellular Polymers in Facilitation of Corrosion: Use of Fourier Transforming Infrared Spectroscopy and Signature Phospholipid Fatty Acid Analysis," in Biologically Induced Corrosion, ed. S.C. Dexter (Houston, TX: NACE, 1985), p. 233.
9. W.P. Iverson, "Microbial Corrosion of Iron," in Microbial Iron Metabolism, ed. J.B. Nieland (New York, NY: Academic Press, 1974), p. 475.
10. G. Hernandez-Duque, A. Pedersen, D. Thierry, M. Hermansson, V. Kucera, "Bacterial Effects of Corrosion of Steel in Seawater," Proc. Microbially Influenced Corrosion and Biodeterioration, eds. N.J. Dowling, M.W. Mittleman, J.C. Danko (Knoxville, TN: University of Tennessee, 1990), p. 241.
11. G. Hernandez, V. Kucera, D. Thierry, A. Pedersen, M. Hermansson, Corrosion 50, 8 (1994): p. 603.
12. C.A. Smith, K.G. Compton, F.H. Coley, Corros. Sci. 13 (1973): p. 677.
13. Z. Lewandowski, T. Funk, F.L. Roe, B.J. Little, "Spatial Distribution of pH at Mild Steel Surfaces Using an Iridium Oxide Microelectrode," in Microbiologically Influenced Corrosion Testing, ASTM STP 1232, eds. J.R. Kearns, B.J. Little (Philadelphia, PA: ASTM, 1994), p. 61.
14. B.B. Jorgensen, N.P. Revsbech, Methods in Enzymology 167 (1988): p. 639.
15. H.L. Wu, R.Q. Yu, Talanta 34, (1987): p. 577.
16. L.F. Jaffe, R. Nuccitelli, J. Cell Biol. 63 (1974): p. 614.
17. J.A. Freeman, P.B. Manis, P.C. Samson, J.P. Wikswo, "Microprocessor Controlled 2- and 3-Dimensional Vibrating Probes with Video Graphics: Biological and Electrochemical Applications," in Ionic Currents in Development, ed. R. Nuccitelli (New York, NY: Liss, 1986), p. 21.
18. K. Nilsson. P. Brodelius. K. Mosbach, Methods in Enzymology 135 (1987): p. 223.
19. L.K. Jang, W. Brand, M. Resong, W. Mainieri, G.G. Geesey, Environ. Prog. 9 (1990): p. 269.
20. O. Smidsrod, A. Haug, Acta Chem. Scand. 22 (1968): p. 1,989.
21. O. Smidsrod, Faraday Disc. Chem. Soc. 57 (1974): p. 263.
22. D. Jones, Principles and Prevention of Corrosion (New York, NY: MacMillian Publishing Co., 1992), p. 189-196.
23. H. Tanaka, M. Matsumura, I.A. Veliky, Biotechnol. Bioeng. 26 (1984): p. 53.
24. F.L. LaQue, Corrosion 13 (1957): p. 303.